

# First VLBI-only TRF/CRF solution based on DGFI-TUM data for ITRF2020

M. Glomsda, M. Seitz, M. Bloßfeld, A. Kehm, M. Gerstl, D. Angermann

**Abstract** DGFI-TUM is an operational Analysis Center (AC) of the International VLBI Service for Geodesy and Astrometry (IVS). In this role, we reprocessed almost all VLBI sessions between 1979 and 2020 for the IVS contribution to the upcoming realization of the International Terrestrial Reference System (ITRS), the ITRF2020. The reprocessed solution contains all requested new geophysical models, including the latest realization of the International Celestial Reference System (ICRS), the ICRF3, as a priori reference frame for the estimated source coordinates. We used our homogeneously reprocessed data to create a preliminary VLBI-only TRF/CRF solution, in which we consistently estimated station positions and velocities, Earth Orientation Parameters (EOP), and radio source positions. It could serve as a new reference for a priori station and source coordinates and will be a good basis for further (inter-technique) combination studies. In this work, we describe the input data, the estimation process, as well as the results of the combination of our session-wise solutions, which has been performed at the normal equation level with our DGFI Orbit and Geodetic parameter estimation Software (DOGS). We also discuss the impact of recently observed and VGOS sessions on the CRF.

**Keywords** VLBI, VGOS, ITRF2020, CRF, consistent estimation

---

Deutsches Geodätisches Forschungsinstitut  
der Technischen Universität München,  
Arcisstraße 21, 80333 München, Germany

## 1 Introduction

The IVS AC DGFI-TUM has contributed to the ITRF2020 with its reprocessed solution *dgf2020a\_woNTAL*. It is based on the latest IERS Conventions of 2010 (Petit and Luzum, 2010) and its updates, including the new models requested for ITRF2020. Furthermore, it contains partial derivatives w.r.t. the radio source coordinates, which was a requirement to be fulfilled by all participating ACs for the first time. The only methodological difference to our current operational IVS contribution, *dgf2020a*, is the missing correction for non-tidal atmospheric loading (at the observation level; Glomsda et al., 2020). Since *dgf2020a\_woNTAL* represents a homogeneous set of almost all 24h VLBI sessions of the last 40 years, including VGOS and mixed-mode observations, we took the opportunity to estimate preliminary VLBI-only TRF/CRF solutions with this data. After all, the consistent estimation of TRF, CRF and EOP is an important goal for the future (Kwak et al., 2018).

## 2 Input data and estimation process

For the TRF/CRF solutions presented here, the session-wise datum-free normal equations of *dgf2020a\_woNTAL* have been combined with the DOGS library CS (“Combination and Solution“; Gerstl et al., 2000). In each session, station coordinates, EOP and radio source coordinates are estimated, after clock and tropospheric parameters have been reduced from the normal equation system. Since all parameters are estimated simultaneously, we obtain a consistent combination of TRF, CRF and EOP.

For the long-term solutions, we estimated a linear TRF, i.e. station coordinates at a reference epoch  $t_0$  as well as constant velocities. For the time being, the EOP are reduced, which means their session-wise information is only implicitly contained in the combined normal equation system. The CRF, on the other hand, is again explicitly estimated. In alignment with the ICRF3 (Charlot et al., 2020), we considered Galactic Aberration (GA), which is an apparent linear motion of the radio sources generated from the acceleration of the solar system barycenter towards the Galactic Center. First, we introduced parameters for source coordinates and velocities at the same reference epoch 2015.0 as used for the ICRF3. Then, the a priori values for the velocities were derived from the formula for GA given in Charlot et al. (2020). Finally, the velocities were fixed to these a priori values and only the corresponding source coordinates were estimated.

To realize the geodetic datum, no-net-translation and no-net-rotation conditions w.r.t. the DTRF2014 as well as no-net-rotation conditions w.r.t. the ICRF3 have been applied to the stations and sources, respectively. As the reference epoch, we chose  $t_0 = 2000.0$ , which is close to the midpoint of the more than 40 years of VLBI observations.

Basically all sessions relevant for the ITRF2020 (i.e. those with at least three stations) have been considered. Only a small fraction of sessions could not be analysed properly and was neglected. Table 1 provides a summary of the input data.

We analysed several TRF/CRF solutions, which will be explained in the upcoming sections. The most critical issue is the inclusion of the VGOS sessions, where newly constructed or converted telescopes are performing broadband observations of the radio sources (e.g., Petrachenko et al., 2009). These VGOS observations and networks are not readily connected with the legacy S/X observations and networks. Hence, one must either introduce local ties between co-located VGOS and legacy antennas, or make use of the mixed-mode sessions, where VGOS and legacy antennas are jointly performing S/X observations. For the future, we plan to also apply local ties at co-locations such as Wettzell or Kokee Park. In the current solutions, however, the networks are tied together by the three mixed-mode sessions only.

**Table 1** Summary of the data included in the distinct CRF/TRF solutions. VCS is the abbreviation for “VLBA Calibrator Survey” (Gordon et al., 2016), and “VCS-like” sessions are those with 1) a VLBA station network plus one additional station and 2) at least 100 observed sources.

time span	1979 - 2020
sessions	6,238
VCS sessions	24 VCS-I + 8 VCS-II
VCS-like sessions	52
VGOS sessions	33
mixed-mode sessions	3
S/X stations [solutions]	114 [158]
VGOS stations [solutions]	8 [8]
datum stations	41 (DTRF2014)
sources	5,044
single-session sources	322
VCS sources	2,458
datum sources	303 (ICRF3 defining sources)
observations	18,266,534
active variables	11,066

### 3 TRF/CRF solutions

#### 3.1 Basic scenario

The basic TRF/CRF solution S1 is the one where all legacy but no VGOS sessions are used. Hence, all estimated coordinates and velocities refer to observations in the S/X-bands.

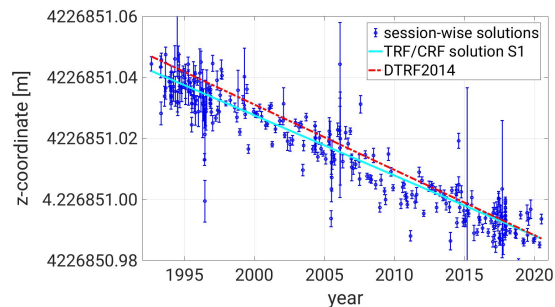


**Fig. 1** The estimated linear motion of the z-coordinate of station NL-VLBA in our basic TRF/CRF solution S1 (solid cyan line), based on the session-wise solutions (blue), and compared to the a priori TRF (dash-dotted red line).

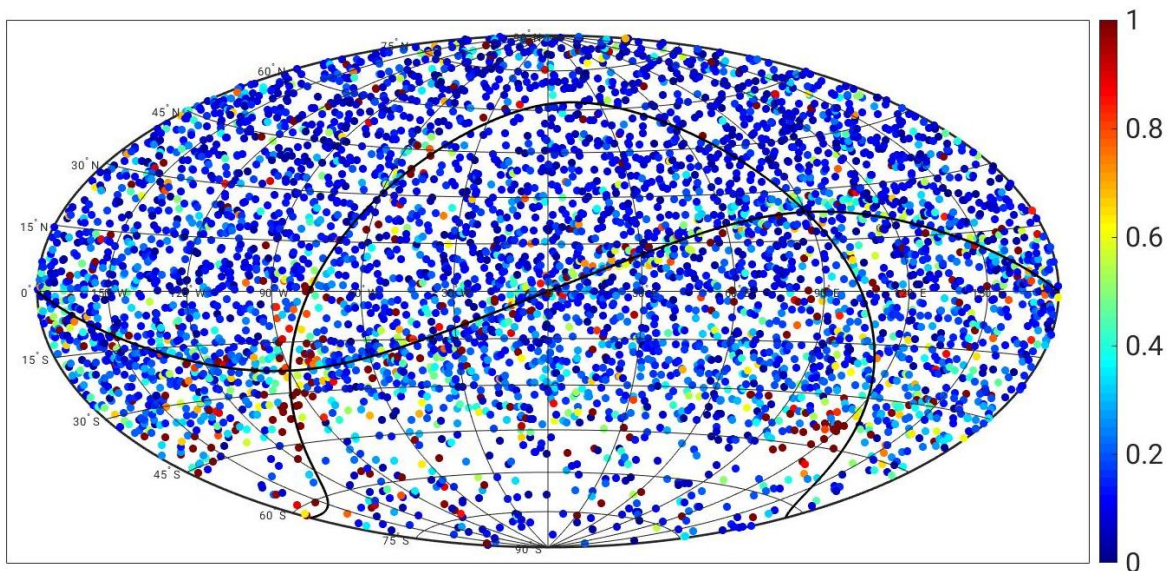


**Fig. 2** Formal errors (in [mas]) of the estimated radio source coordinates in the basic TRF/CRF solution S1.

### 3.1.1 TRF

When comparing the estimated linear station coordinates with the time series of single-session coordinates, we usually found a good fit. On the other hand, a 14-parameter Helmert transformation w.r.t. the DTRF2014, DGFI-TUM’s latest realization of the ITRS (Seitz et al., 2016), revealed a quite significant change in network geometry for transformation epoch 2000.0, which must be analysed in more detail. At the very least, our TRF/CRF solution has been created from six years of additional data, which will likely lead to different station motions, cf. Fig. 1. The new models used for ITRF2020, such as the gravitational deformation of six antennas and the updated mean pole formula, might also have some influence.

### 3.1.2 CRF

Figure 2 shows the estimated radio source positions  $p = (\alpha, \delta)$  at epoch 2015.0 on the celestial sphere together with their formal errors (standard deviations)

$$\sigma_p = \sqrt{\sigma_\delta^2 + [\sigma_\alpha \cdot \cos(\delta)]^2}, \quad (1)$$

where  $\alpha$  and  $\delta$  represent the right ascension and the declination of a radio source, respectively. The

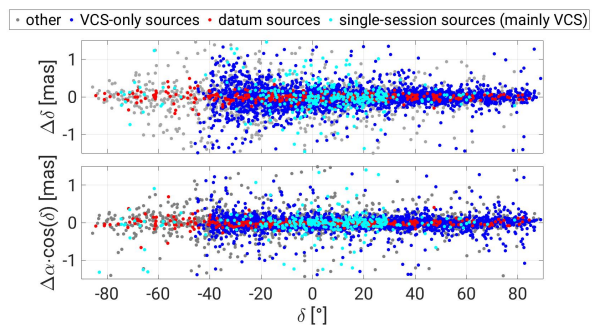


**Fig. 3** Changes in declination  $\delta$  and right ascension  $\alpha$  for the sources estimated in our basic TRF/CRF solution S1 w.r.t. their a priori values from the ICRF3, separated by source type.

errors are generally larger at the Galactic (impeded observations through the Milky Way) and the Ecliptic plane (many single-session sources). The plot looks very similar to the S/X-band component of the ICRF3 (Charlot et al., 2020).

In Fig. 3, the changes in the declinations and right ascensions of the sources w.r.t. the ICRF3 are plotted (separated by particular source types). There are no systematic deviations, but we can observe that the datum sources have the smallest differences (showing a good agreement with ICRF3), and that the single-session sources are concentrated at declinations  $|\delta| < 23.44^\circ$  (Ecliptic).

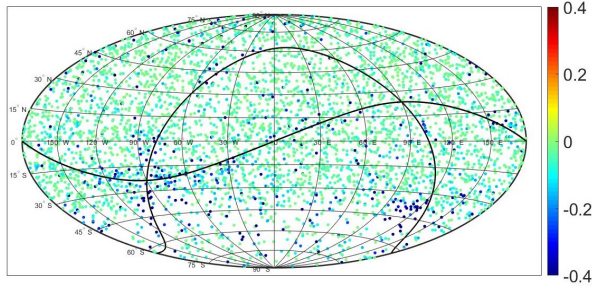


**Fig. 4** Changes in standard deviations (in [mas]) when adding the data of the years 2018–2020 to the TRF/CRF solution.

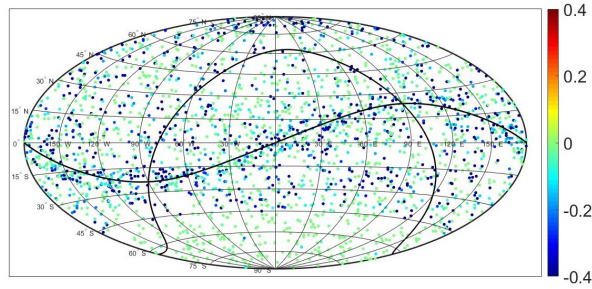


**Fig. 5** Changes in standard deviations (in [mas]) when adding the VCS and VCS-like sessions to the TRF/CRF solution. The set of sources is much smaller without the VCS (-like) sessions.

### 3.2 Impact of post-ICRF3 period

The ICRF3 was generated from VLBI data up to the beginning of 2018 (Charlot et al., 2020). Hence, solution S1 contains three more years of data. To investigate the corresponding impact, we computed another TRF/CRF solution, S2, without the sessions of the years 2018–2020. Figure 4 shows the changes in the source positions’ standard deviations of Eq. (1) when including these sessions, i.e. when moving from solution S2 to solution S1. As expected, the additional data improves the formal errors of all estimated radio source positions. The mean and median decrease in standard deviations are about  $-0.05$  and  $-0.03$  mas, respectively.

In particular, additional VCS or VCS-like sessions were scheduled during the last three years. These are specifically designed to improve the formal errors of rarely observed radio sources. To confirm their benefit, we computed the TRF/CRF solution S3, where all (i.e. also before 2018) VCS and VCS-like sessions are neglected. In Fig. 5, we see that the standard deviations of all remaining radio sources actually decrease when the VCS (-like) sessions are included, especially near

the Ecliptic plane. The mean and median drop in formal errors are about  $-0.2$  and  $-0.05$  mas, respectively.

### 3.3 Impact of VGOS observations

It is of particular interest how the new VGOS sessions affect the TRF/CRF solution. As mentioned before, we did not apply local ties between co-located VGOS and legacy antennas, but only used the mixed-mode sessions for the connection of the two distinct networks. And there is another issue when including the VGOS sessions: the observed frequency bands differ w.r.t. the legacy S/X sessions. Since the structure of radio sources changes with frequency (e.g., Petráchenko et al., 2009), the source positions will probably deviate between VGOS and legacy observations.

To investigate this, we created two further TRF/CRF solutions: in S4, there is a single parameter for each source coordinate, irrespective of whether the source is observed in a VGOS or a legacy session. In S5, on the other hand, there contingently are two right ascension and two declination parameters for each source: one referring to the VGOS observations, and one referring to the legacy observations.

#### 3.3.1 CRF

Compared to solution S1, the impact of the VGOS sessions on the radio source positions is rather small in both cases. However, when comparing the formal position errors between the solutions S4 and S5, we find that the standard deviations of the coordinates estimated from the VGOS sessions only significantly deteriorate (see Fig. 6), while those estimated from the legacy sessions are hardly affected by the separation (see Fig. 7). This is no surprise, as the number of VGOS sessions is very small. Nevertheless, the separation might be justified by the frequency-dependent source structure, and hence the increased formal errors must be accepted until more VGOS data is available.

#### 3.3.2 TRF

The estimated station motions are not separated for VGOS and legacy sessions. Even though some stations

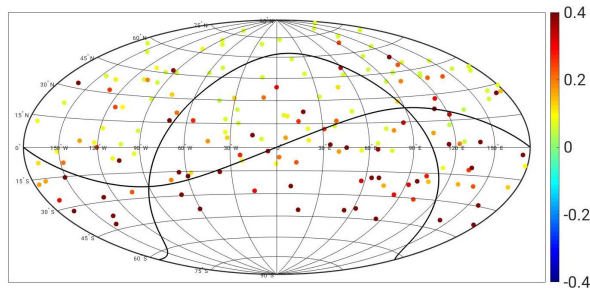


**Fig. 6** Changes in standard deviations (in [mas]) when separating the estimated source positions for VGOS and legacy sessions: VGOS session parameters.

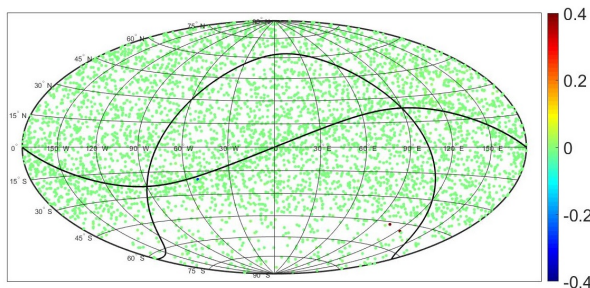


**Fig. 7** Changes in standard deviations (in [mas]) when separating the estimated source positions for VGOS and legacy sessions: legacy session parameters.

have switched from S/X legacy to VGOS broadband receivers in the past (e.g., WESTFORD and ISHIOKA), their reference points are supposed to remain the same. Nevertheless, to investigate whether the new observations have an impact on the station network, we analysed 14-parameter Helmert transformations between our basic solution S1 and the two VGOS solutions S4 and S5, as well as the transformation between S4 and S5 themselves.

In Table 2, we list the transformation residuals for ISHIOKA. It was striking, because there is a large residual in the up components when the source coordinates are separated by frequency (S5), which disappears if VGOS and legacy positions are equalized (S4). The residuals of the VGOS stations generally are quite large in both cases, which might implicate that the small number of VGOS sessions is only weakly tied to the legacy network by the mixed-mode sessions. Station heights seem to be affected most, but there is no unique pattern and hence no obvious VGOS-related scale issue, either. All in all, however, there are subtle effects created by the inclusion of the VGOS data.

**Table 2** Residuals of the two solutions A01 and A02 for VGOS station ISHIOKA in the 14-parameter Helmert-transformations. N, E and U represent the coordinate residuals in North, East and up direction, respectively. The unit is [mm]. VN, VE and VU represent the velocity residuals in North, East and up direction, respectively. The unit is [mm/yr].

transformation	solnr	N	E	U	VN	VE	VU
S1 to S4	A01	-0.44	-1.17	0.40	0.03	0.08	-0.02
	A02	-4.53	0.36	-3.48	0.24	-0.01	0.18
S1 to S5	A01	0.50	-0.19	-7.07	-0.03	0.01	0.43
	A02	-3.38	0.39	-2.28	0.18	-0.02	0.12
S5 to S4	A01	-0.94	-0.97	7.48	0.06	0.06	-0.45
	A02	-1.14	-0.03	-1.20	0.06	0.01	0.07

### 3.4 Conclusion

We have estimated several consistent VLBI-only TRF/CRF solutions from our ITRF2020-contribution *dgf2020a\_woNTAL*, which look promising in the first place. Nevertheless, some aspects need further investigation, e.g. the proper inclusion and corresponding effects of the VGOS observations.

### References

- Charlot P., Jacobs C.S., et al. (2020): The third realization of the International Celestial Reference Frame by very long baseline interferometry. *Astronomy & Astrophysics*, 644.
- Gerstl M., Kelm R., Müller H., and Ehrnsperger W. (2000): DOGS-CS – Kombination und Lösung großer Gleichungssysteme. *Internal Report*, DGFI-TUM.
- Glomsda M., Bloßfeld M., Seitz M., and Seitz F. (2020): Benefits of non-tidal loading applied at distinct levels in VLBI analysis. *Journal of Geodesy*, Vol. 94 (90).
- Gordon D., Jacobs C., Beasley A., et al. (2016): Second Epoch VLBA Calibrator Survey Observations: VCS-II. *The Astronomical Journal*, Vol. 151, No. 6.
- Kwak Y., Bloßfeld M., Schmid R., Angermann D., Gerstl M., and Seitz M. (2018): Consistent realization of Celestial and Terrestrial Reference Frames. *Journal of Geodesy*, Vol. 92, pp. 1047–1061.
- Petit G. and Luzum B. (2010): IERS Technical Note 36, Version 1.3.0. *Verlag des Bundesamts für Kartographie und Geodäsie*, Frankfurt am Main.
- Petrachenko B., Niell A., et al. (2009): Design aspects of the VLBI2010 system. Progress report of the VLBI2010 committee. *NASA/TM-2009-214180*.
- Seitz M., Bloßfeld M., Angermann D., Schmid R., Gerstl M., and Seitz F. (2016): The new DGFI-TUM realization of the ITRS: DTRF2014 (data). <http://doi.pangaea.de/10.1594/PANGAEA.864046>